Eddy Currents Induced in Two Parallel Round Conductors

Tomasz Szczegielniak [1], Paweł Jabłoński [1], Dariusz Kusiak [1], and Zygmunt Piątek [2]

[1] Department of Automation, Electrical Engineering and Optoelectronics, Faculty of Electrical Engineering
Czestochowa University of Technology, Armii Krajowej 17, 42-200 Czestochowa, Poland
tomasz.szczegielniak@pcz.pl, pawel.jablonski@pcz.pl, dariusz.kusiak@pcz.pl

[2] Czestochowa University of Technology, Poland
zygmunt.piatek@interia.pl

Abstract **—** The paper presents a method of analysis of eddy currents induced in a system of two parallel round conductors by a transverse alternating magnetic field generated by a current in one of them. The magnetic field is represented by means of magnetic vector potential as expansion into Fourier series. Using the Laplace and Helmholtz equations as well as the classical boundary conditions we determine analytically the current density induced due to the proximity effect. Power transmission lines with round conductors are widely used in distribution networks. Therefore, although the paper is theoretical, the determination of electromagnetic parameters of the power transmission lines is of huge practical significance.

Index Terms **—** Current density, eddy currents, proximity effect, round conductor.

I. INTRODUCTION

A system of two or more round wires is very often used in power transmission lines. For example, in a three phase cable line there are often three round wires as a three-core cable or three single-core cables in the trefoil or the flat formation [1]. In each conductor, eddy currents are induced by magnetic field generated by neighboring alternating currents. The eddy currents induced in the conductors affect considerably the physical quantities related with the wires, such as impedances, electromagnetic field and power losses [2-4].

In order to calculate the current density induced in a twin line built from solid conductors of circular cross section a series of analytical [5-9] and numerical methods [10-13] are used. One of them consists in replacing the source wire with a current filament placed on the axis of the wire. Then the eddy currents induced in the second round wire may be determined analytically, e.g., they can be deduced from the solution for tubular, screen [14-16] after assuming that the inner radius equals zero.

In this paper we propose the method of successive approximations for calculating eddy currents induced in the round conductor using the magnetic vector potential. The determined current densities can be used to calculate impedances, magnetic field and power losses resulting from induced eddy currents.

The geometry of the system under consideration is shown in Fig. 1. The radii of the conductors are R_1 and R_2 respectively and the distance between the conductor axes is d. A sinusoidal current of angular frequency ω and complex r.m.s. value $\underline{I}_1$ flows through the first (source) conductor.

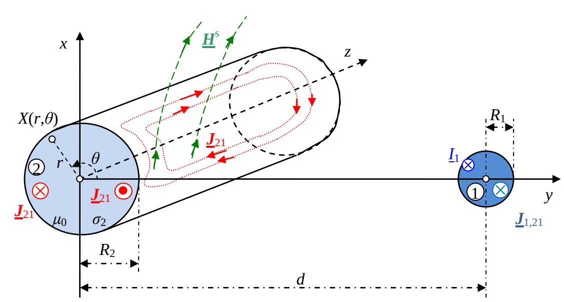

Fig. 1. Eddy currents induced in a round conductor (on the left) by the magnetic field of the neighboring conductor (on the right).

There are two kinds of induced eddy currents. The first one consists in inducing eddy currents $\underline{\mathbf{J}}_{21}(r,\ \theta) = \mathbf{1}_z\underline{J}_{21}(r,\ \theta)$ in the second conductor by time harmonic magnetic field $\underline{\mathbf{H}}^s(r_{XY})$ ("source field") generated by current $\underline{I}_1$ in the first conductor. The second one is the current density $\underline{J}_{1,21}(\rho,\ \varphi)$ induced in the first tubular conductor by previously induced current density $\underline{J}_{21}(r,\ \theta)$.

In [9] current $\underline{I}_1$ in the first round conductor was assumed to be located at the wire axis as a filament current. Then the magnetic field of the first conductor was represented by means of the magnetic vector

Submitted On: July 26, 2019
Accepted On: October 23, 2019

potential expanded into Fourier series. In the non-conducting external region, the Laplace equation was used to determine the magnetic field strength with taking into account the reverse reaction of the eddy currents induced in the considered conductor. The Helmholtz equation supplemented with classical boundary conditions was used to determine the eddy current density. The final formulas obtained in this procedure are as follows:

- The current density in the second round conductor induced by current $\underline{I}_1$ flowing through the first one:

$$\underline{J}_{21}(r,\theta) = -\frac{\underline{\Gamma}_2\,\underline{I}_1}{\pi R_2}\sum_{n=1}^{\infty}\left(\frac{R_2}{d}\right)^n \frac{I_n(\underline{\Gamma}_2 r)}{I_{n-1}(\underline{\Gamma}_2 R_2)}\cos n\theta\,, \quad (1)$$

  in which I_{n-1} and I_{n+1} are the modified Bessel functions of the first kind of orders n–1and n, respectively;

- The complex propagation constant:

$$\underline{\Gamma}_2 = \sqrt{\mathrm{j}\omega\mu_2\sigma_2} = \sqrt{\omega\mu_2\sigma_2}\,\exp\left(\mathrm{j}\frac{\pi}{4}\right), \quad (2)$$

  where σ_2 is the conductivity and μ_2 is the permeability of the second round conductor;

- By analogy, the current density in the first tubular conductor induced by current $\underline{I}_2$ flowing through the second one is:

$$\underline{J}_{12}(r,\theta) = -\frac{\underline{\Gamma}_1\underline{I}_2}{\pi R_1}\sum_{n=1}^{\infty}\left(-\frac{R_1}{d}\right)^n \frac{I_n(\underline{\Gamma}_1 r)}{I_{n-1}(\underline{\Gamma}_1 R_1)}\cos n\theta\,, \quad (3)$$

  in which the complex propagation constant of the first round conductor is defined by the formula:

$$\underline{\Gamma}_1 = \sqrt{\mathrm{j}\omega\mu_1\sigma_1} = \sqrt{\omega\mu_1\sigma_1}\,\exp\left(\mathrm{j}\frac{\pi}{4}\right), \quad (4)$$

  where σ_1 is the conductivity and μ_1 the permeability of the first round conductor.

However, it should be realized that the induced current given by Eq. (1), from now on denoted as $\underline{\boldsymbol{J}}_{21}^{(1)}(r,\theta)$ and called the first approximation of the total induced current density in wire 2, induces also a current of density $\underline{\boldsymbol{J}}_{1,21}^{(1)}(\rho,\varphi)$ in the first conductor, which in turn induces the current density $\underline{\boldsymbol{J}}_{21}^{(2)}(r,\theta)$ which adds to $\underline{\boldsymbol{J}}_{21}^{(1)}(r,\theta)$ in the second conductor. Hence, the current density in the second conductor can be regarded as the following sum:

$$\underline{\boldsymbol{J}}_{21}(r,\theta) = \sum_{m=1}^{\infty}\underline{\boldsymbol{J}}_{21}^{(m)}(r,\theta)\,, \quad (5)$$

where $\underline{\boldsymbol{J}}_{21}^{(m)}$ is the m^{th} term of current density induced in the second round conductor. In previous works, e.g., [9, 14-16], the focus was directed on $\underline{\boldsymbol{J}}_{21}^{(1)}(r,\theta)$. In this paper, the aim is to determine the second approximation.

II. THE FIRST APPROXIMATION

Let us consider two round parallel conductors. Conductor 1 of conductivity σ_1 and radius R_1 leads a time harmonic current of r.m.s. $\underline{I}_1$ and angular frequency ω. The second conductor of conductivity σ_2 and radius R_2 is affected by the magnetic field generated by the first conductor (Fig. 2).

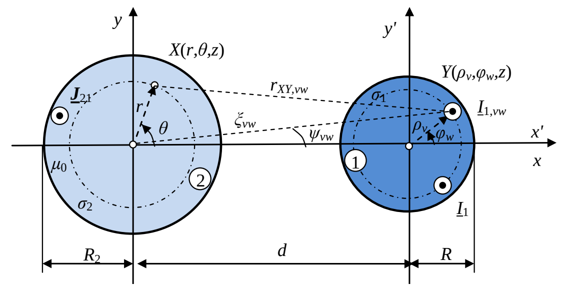

Fig. 2. Conductor 2 (on the left) in non-uniform magnetic field due to current $\underline{I}_1$ in conductor 1 (on the right).

In general, the current density in the first conductor is non-uniform. Therefore, the cross section of the first round conductor is divided into elementary segments of radial dimension:

$$\Delta\rho = \frac{R_1}{V}\,, \quad (6)$$

and angular span:

$$\Delta\varphi = \frac{2\pi}{W}\,, \quad (7)$$

as shown in Fig. 3.

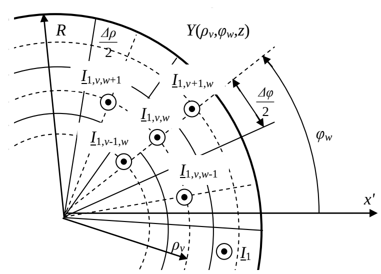

Fig. 3. Division of conductor 1 into segments.

For low frequency, we can assume that the total current $\underline{I}_1$ is represented by a set of $V\times W$ filament currents distributed discreetly at points $Y(\rho_v, \varphi_w)$ in cylindrical coordinates system determined by radius:

$$\rho_v = (2v-1)\frac{\Delta\rho}{2}\,, \quad (8)$$

and angle:

$$\varphi_w = (2w-1)\frac{\Delta\varphi}{2}\,, \quad (9)$$

where v = 1, 2, …, V and w = 1, 2, …, W. The area of such a segment equals:

$$S_{vw} = \rho_v\,\Delta\rho\,\Delta\varphi\,. \quad (10)$$

Then the current in segment (v, w) is:

$$\underline{I}_{1vw}^{(0)}(\rho_v,\varphi_w)=S_{vw}\underline{J}_1^{(0)}(\rho_v,\varphi_w)\,, \tag{11}$$

where $\underline{J}_1^{(0)}$ is an initial approximation of current density in conductor 1. For example, it can be a DC density as follows:

$$\underline{J}_1^{(0)}=\frac{\underline{I}_1}{\pi R_1^2}\,, \tag{12}$$

but it is more reasonable to use formula with the skin effect taken into account as follows:

$$\underline{J}_1^{(0)}=\frac{\underline{\Gamma}_2\,\underline{I}_2}{2\pi\,R_2}\frac{I_0(\underline{\Gamma}_2 r)}{I_1(\underline{\Gamma}_2 R_2)}\,. \tag{13}$$

The magnetic vector potential generated by current $\underline{I}_1$ has only one component parallel to the conductor's axis (z component) as follows:

$$\underline{\boldsymbol{A}}^s(r_{XY})=\mathbf{1}_z\underline{A}^s(r_{XY,vw})\,. \tag{14}$$

It is the source potential with respect to the first conductor and it is given by following formula:

$$\underline{A}^s(r_{XY})=\sum_{v=1}^{V}\sum_{w=1}^{W}\frac{\mu_0\underline{I}_{1,vw}^{(0)}}{2\pi}\ln\frac{1}{r_{XY,vw}}+\underline{A}_0\,, \tag{15}$$

where the constant $\underline{A}_0$ can be freely assumed.

The above magnetic vector potential can be expressed in local cylindrical system of co-ordinates (r, θ, z) related with the second conductor. From Fig. 2 it follows that:

$$r_{XY,vw}^2=r^2+\xi_{vw}^2-2r\xi_{vw}\cos(\theta-\psi_{vw})\,, \tag{16}$$

where

$$\xi_{vw}^2=\rho_v^2+d^2+2\rho_v d\cos\varphi_w\,, \tag{17}$$

and

$$\psi_{vw}=\arcsin\left(\frac{\rho_v}{\xi_{vw}}\sin\varphi_w\right). \tag{18}$$

Thus, the total vector potential becomes:

$$\underline{A}^w(r_{XY})=\sum_{v=1}^{V}\sum_{w=1}^{W}\frac{\mu_0\underline{I}_{1,vw}^{(0)}}{2\pi}\times\\ \times\ln\frac{1}{\sqrt{r^2+\xi_{vw}^2-2r\xi_{vw}\cos(\theta-\psi_{vw})}}+\underline{A}_0. \tag{19}$$

The expression under the square root can be rewritten as follows:

$$\frac{r_{XY,vw}{}^2}{\xi_{vw}^2}=1+\left(\frac{r}{\xi_{vw}}\right)^2-2\frac{r}{\xi_{vw}}\cos(\theta-\psi_{vw})\,. \tag{20}$$

Hence,

$$\ln\frac{r_{XY,vw}}{\xi_{vw}}=\frac{1}{2}\ln\left[1+\left(\frac{r}{\xi_{vw}}\right)^2-2\frac{r}{\xi_{vw}}\cos(\theta-\psi_{vw})\right], \tag{21}$$

and by expanding the right-hand side of equation (21) into Fourier series[1] it follows that:

$$\ln\frac{r_{XY,vw}}{\xi_{vw}}=-\sum_{n=1}^{\infty}\frac{1}{n}\left(\frac{r}{\xi_{vw}}\right)^n\cos n(\theta-\psi_{vw})\,, \tag{22}$$

for $r<\xi_{vw}$. Hence,

$$\ln\frac{1}{r_{XY,vw}}=\ln\frac{1}{\xi_{vw}}+\sum_{n=1}^{\infty}\frac{1}{n}\left(\frac{r}{\xi_{vw}}\right)^n\cos n(\theta-\psi_{vw})\,, \tag{23}$$

and the magnetic vector potential (19) at point $X(r,\theta)$ such that $r<\xi_{vw}$ can be rewritten as follows:

$$\underline{A}^s(r,\theta)=\frac{\mu_0}{2\pi}\sum_{v=1}^{V}\sum_{w=1}^{W}\underline{I}_{1,vw}^{(0)}\left[\ln\frac{1}{\xi_{vw}}+\right.\\ \left.+\sum_{n=1}^{\infty}\frac{1}{n}\left(\frac{r}{\xi_{vw}}\right)^n\cos n(\theta-\psi_{vw})\right]+\underline{A}_0. \tag{24}$$

In order to determine the density of the current induced in conductor 2 we may apply the analytical procedure shown in [9, 14-16]. Finally, the first approximation of the current density induced in the second round conductor by the current $\underline{I}_1$ in the first round conductor takes the following form:

$$\underline{J}_{21}^{(1)}(r,\theta)=-\frac{\underline{\Gamma}_2}{\pi R_2}\sum_{v=1}^{V}\sum_{w=1}^{W}\underline{I}_{1,vw}^{(0)}\times\\ \times\sum_{n=1}^{\infty}\left(\frac{R_2}{\xi_{vw}}\right)^n\frac{I_n(\underline{\Gamma}_2 r)}{I_{n-1}(\underline{\Gamma}_2 R_2)}\cos n(\theta-\psi_{vw}). \tag{25}$$

The distributions of magnitude of this current density on the surface of this conductor for various discretization parameters are shown in Fig. 4.

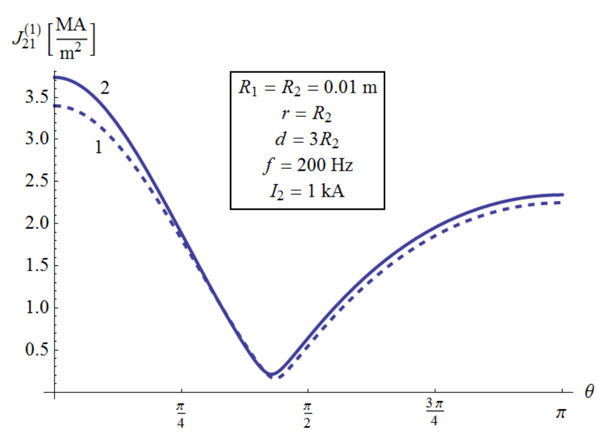

Fig. 4. Magnitude of the first approximation of the current density given by (25) for $V = 4$ and $W = 2$ (solid curve 1), $W = 180$ (dotted curve 2).

[1] Reference [17] provides formula (1.514):

$$\ln(1+x^2-2x\cos\alpha)=-2\sum_{n=1}^{\infty}\frac{1}{n}x^n\cos n\alpha\,.$$

The results calculated via (25) marginally depend on the number of radial division (V). Their dependence on angular division (W) is rather slight – in practice, the results remain the same for $W > 18$. The magnitude of the density of the induced eddy currents acquires the highest values at the point closest to the neighboring conductor, i.e., for $\theta = 0°$. It strongly depends on frequency, which is shown in Fig. 5.

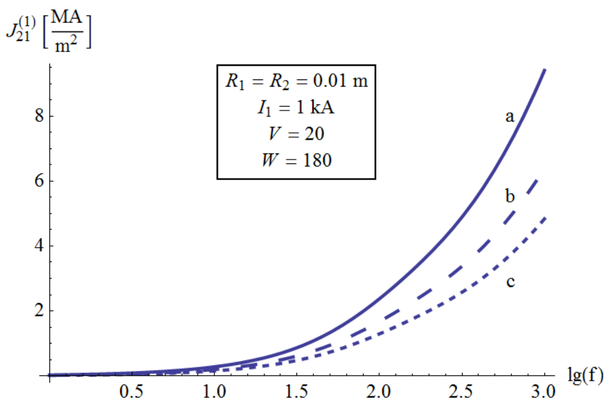

Fig. 5. Magnitude of current density given by (25) at point $r = R_1$, $\theta = 0°$ vs. frequency f for $d = 3R_2$ (solid curve a), $d = 4R_2$ (dashed curve b), $d = 5R_2$ (dotted curve c); calculations performed for $V = 20$ and $W = 180$.

The same results are obtained when applying (1). So, the first approximation given by (25) describes the current density induced in conductor 2 as if current $\underline{I}_1$ was located on the axis of conductor 1.

The first approximation of current density, $\underline{J}_{21}^{(1)}(r,\theta)$, strongly depends on the distance d, which is shown in Fig. 6.

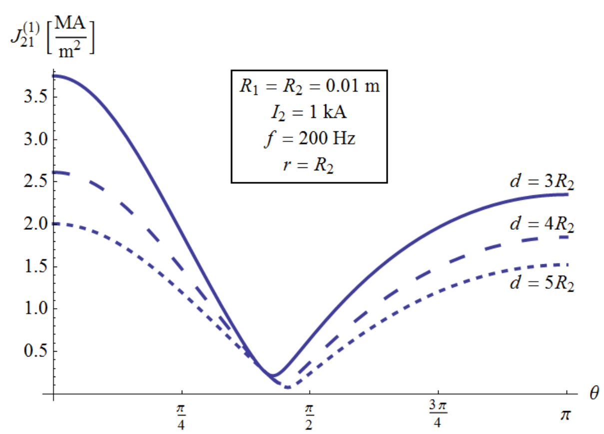

Fig. 6. Magnitude of current density given by (25) on the surface of conductor 2 for various distances d.

The argument of current density, $\varphi_{21}^{(1)}(r,\theta)$, also depends on distance d – see Fig. 7.

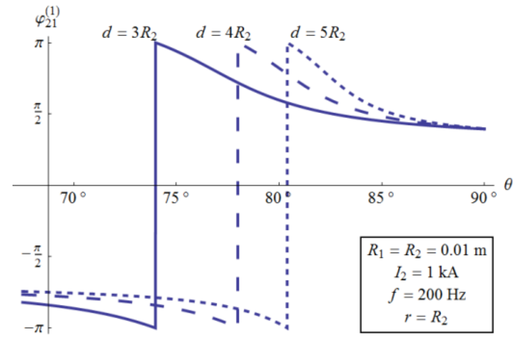

Fig. 7. Argument of the current density given by (25) on the surface of conductor 2 for various distances d.

A similar procedure can be applied, when the second conductor carries current $\underline{I}_2$ which induces eddy currents in the first conductor (Fig. 8).

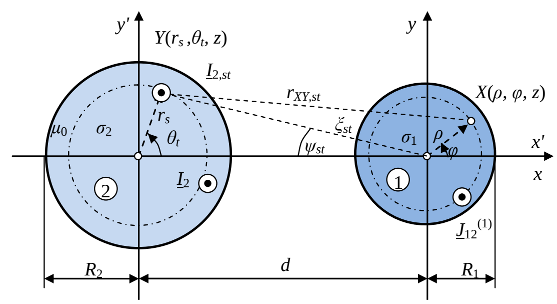

Fig. 8. Quantities used for calculating the current density induced in conductor 1 due to magnetic field generated by current $\underline{I}_2$ in conductor 2.

In general, the current density in the second conductor is non-uniform as well. Therefore, the cross section of conductor 2 is divided into polar segments of radial dimension:

$$\Delta r = \frac{R_2}{S}, \tag{26}$$

and angular span:

$$\Delta\theta = \frac{2\pi}{T}, \tag{27}$$

as shown in Fig. 9.

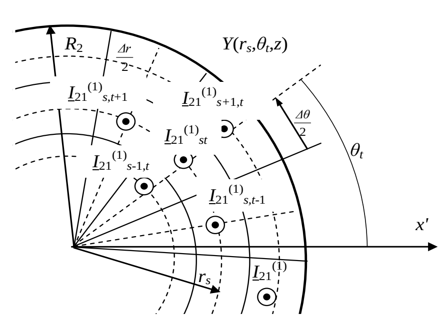

Fig. 9. Division of conductor 2 into polar segments.

Current of density $\underline{J}_2(r_s,\ \theta_t)$ is approximated by a system of filaments located at points $Y(r_s,\ \theta_t)$ in the cylindrical co-ordinates associated with conductor 2, where:

$$r_s = (2s-1)\frac{\Delta r}{2}\,, \tag{28}$$

and

$$\theta_t = (2t-1)\frac{\Delta\theta}{2}\,, \tag{29}$$

where $s = 1, 2, \ldots, S$ and $t = 1, 2, \ldots, T$.

The area of the segment equals:

$$S_{st} = r_s \Delta r \Delta\theta\,. \tag{30}$$

Then from Fig. 8 it follows that:

$$\begin{aligned} r_{XY,st}^2 &= \rho^2 + \xi_{st}^2 + 2\rho\xi_{st}\cos(\varphi+\psi_{st}) = \\ &= \rho^2 + \xi_{st}^2 - 2\rho\xi_{st}\cos(\pi-\varphi-\psi_{st}), \end{aligned} \tag{31}$$

where

$$\xi_{st}^2 = r_s^2 + d^2 - 2\,r_s d\cos\theta_t\,, \tag{32}$$

and

$$\psi_{st} = \arcsin\left(\frac{r_s}{\xi_{st}}\sin\theta_t\right). \tag{33}$$

Hence, the current in each segment equals:

$$\begin{aligned} \underline{I}_{2,st}^{(0)} &= S_{st}\,\underline{J}_2^{(0)}(r=r_s,\theta=\theta_t) = \\ &= \frac{\underline{\Gamma}_2\,\underline{I}_2 r_s \Delta r\Delta\theta}{2\pi R_2}\,\frac{I_0(\underline{\Gamma}_2 r_s)}{I_1(\underline{\Gamma}_2 R_2)}. \end{aligned} \tag{34}$$

Applying the procedure given above in (19)-(25) for the second conductor, the following formula representing the first approximation of the eddy current density induced in the first conductor by current $\underline{I}_2$ in conductor 2 is obtained:

$$\begin{aligned} \underline{J}_{12}^{(1)}(\rho,\varphi) &= -\frac{\underline{\Gamma}_1}{\pi R_1}\sum_{s=1}^{S}\sum_{t=1}^{T}\sum_{n=1}^{\infty}\underline{I}_{2,st}^{(0)}(-1)^n\left(\frac{R_1}{\xi_{st}}\right)^n \times \\ &\times \frac{I_n(\underline{\Gamma}_1\rho)}{I_{n-1}(\underline{\Gamma}_1 R_1)}\cos n(\varphi+\psi_{st}) = \\ &= J_{12}^{(1)}(\rho,\varphi)\exp[\mathrm{j}\varphi_{12}^{(1)}(\rho,\varphi)]. \end{aligned} \tag{35}$$

In case of two identical conductors the distributions of current density magnitude and argument will be symmetrical to those given by (25) – see Fig. 10 and Fig. 11.

The proposed method was compared with finite element method (FEM) – Table 1.

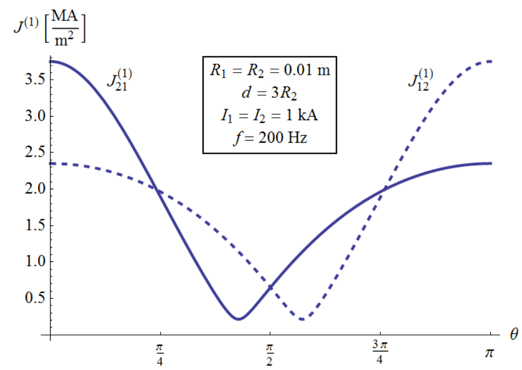

Fig. 10. Distributions of magnitude of eddy current densities given by (25) on the surfaces of two same conductors due to currents in the neighboring conductor.

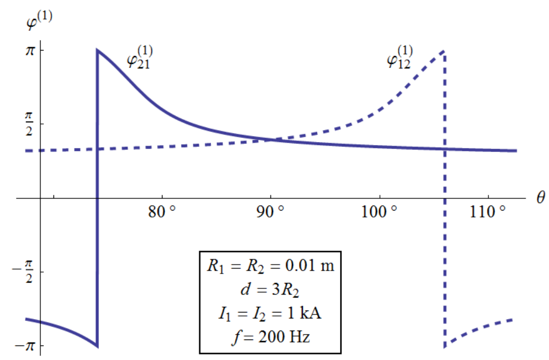

Fig. 11. Distributions of argument of eddy current densities given by (25) on the surfaces of two same conductors due to currents in the neighboring conductor.

Table 1: Magnitudes of the total current densities induced at characteristic points on the surfaces of two same conductors arranged in a twin line

$R_1 = R_2 = 0.01$ m; $d = 3R_2$; $\sigma_1 = \sigma_2 = 55\cdot10^6$ S·m^{-1} $I = 1$ kA; $f = 200$ Hz		**Proposed Method**	**FEM**
		$J^{(1)}$ kA·m^{-2}	J kA·m^{-2}
Conductor 1 $\rho = R_1$	$\varphi = 0$	2352	2321
	$\varphi = \pi/2$	650	650
	$\varphi = \pi$	3753	3714
Conductor 2 $r = R_2$	$\theta = 0$	3753	3714
	$\theta = \pi/2$	650	650
	$\theta = \pi$	2352	2321

III. THE SECOND APPROXIMATION

The current of density $\underline{J}_{21}^{(1)}(r,\theta)$ induced in the second conductor by current by current $\underline{I}_1$ induces itself current of density $\underline{J}_{1,21}^{(1)}(\rho,\varphi)$ in the first conductor (this can be considered as a reverse reaction). However, $\underline{J}_{21}^{(1)}(r,\theta)$ is non-uniformly distributed - see (25) and Figs. 6 and 10. To determine $\underline{J}_{1,21}^{(1)}(\rho,\varphi)$, a set of filaments arranged in polar grid as in Fig. 9 can be used. The procedure is quite similar to that described by (26)-(35) with that difference that $\underline{J}_{21}^{(1)}(r,\theta)$ is used instead of $\underline{J}_2^{(0)}$. Hence,

$$\underline{I}_{21st}^{(1)} = S_{st}\underline{J}_{21}^{(1)}(r=r_s,\theta=\theta_t)\,, \tag{36}$$

and the reverse reaction in conductor 1 can be written as:

$$\underline{J}_{1,21}^{(1)}(\rho,\varphi) = -\frac{\underline{\Gamma}_1}{\pi R_1}\sum_{s=1}^{S}\sum_{t=1}^{T}\sum_{n=1}^{\infty}\underline{I}_{21st}^{(1)}(-1)^n \times \left(\frac{R_1}{\xi_{st}}\right)^n \frac{I_n(\underline{\Gamma}_1\rho)}{I_{n-1}(\underline{\Gamma}_1 R_1)}\cos n(\varphi+\psi_{st}). \tag{37}$$

The induced current of density $\underline{J}_{1,21}^{(1)}(\rho,\varphi)$ is then a source of further magnetic field which induces secondary eddy currents in conductor 2. To evaluate their density, the same polar grid as in Fig. 3 can be used, but this time the currents associated with the filaments are as follows:

$$\underline{I}_{1,21vw}^{(1)} = S_{vw}\underline{J}_{1,21}^{(1)}(\rho=\rho_v,\varphi=\varphi_w)\,. \tag{38}$$

Each such a current contributes to the second correction to the eddy currents in a similar way as given by (25) so that:

$$\underline{J}_{21}^{(2)}(r,\theta) = -\frac{\underline{\Gamma}_2}{\pi R_2}\sum_{v=1}^{V}\sum_{w=1}^{W}\sum_{n=1}^{\infty}\underline{I}_{1,21vw}^{(1)} \times \left(\frac{R_2}{\xi_{vw}}\right)^n \frac{I_n(\underline{\Gamma}_2 r)}{I_{n-1}(\underline{\Gamma}_2 R_2)}\cos n(\theta-\psi_{vw}). \tag{39}$$

A similar procedure can be repeated for the second correction in conductor 1. To avoid extensive repetitions, only the key formulas are given below:

$$\underline{I}_{12vw}^{(1)} = S_{vw}\underline{J}_{12}^{(1)}(\rho=\rho_v,\varphi=\varphi_w)\,, \tag{40}$$

$$\underline{J}_{2,12}^{(1)}(r,\theta) = -\frac{\underline{\Gamma}_2}{\pi R_2}\sum_{v=1}^{V}\sum_{w=1}^{W}\sum_{n=1}^{\infty}\underline{I}_{12vw}^{(1)} \times \left(\frac{R_2}{\xi_{vw}}\right)^n \frac{I_n(\underline{\Gamma}_2 r)}{I_{n-1}(\underline{\Gamma}_2 R_2)}\cos n(\theta-\psi_{vw}), \tag{41}$$

$$\underline{I}_{2,12st}^{(1)} = S_{st}\underline{J}_{2,12}^{(1)}(r=r_s,\theta=\theta_t)\,, \tag{42}$$

and finally,

$$\underline{J}_{12}^{(2)}(\rho,\varphi) = -\frac{\underline{\Gamma}_1}{\pi R_1}\times\sum_{s=1}^{S}\sum_{t=1}^{T}\sum_{n=1}^{\infty}\underline{I}_{2,12st}^{(1)} \times \left(\frac{R_1}{\xi_{st}}\right)^n (-1)^n \frac{I_n(\underline{\Gamma}_1\rho)}{I_{n-1}(\underline{\Gamma}_1 R_1)}\cos n(\varphi+\psi_{st}). \tag{43}$$

In a similar way the corrections of third and higher orders can be found. But numerical calculations show they are very low compared to the first one even for high frequency. So, they can be often neglected.

IV. THE TOTAL INDUCED CURRENT DENSITY

The total current density induced in the neighboring conductor is a sum of all the corrections. As mentioned above, the third and higher order terms can be often neglected so that the results can be limited to the first two terms. Hence, the total induced current density can be approximated as follows:

- In conductor 2:

$$\underline{J}_{21}(r,\theta) = \underline{J}_{21}^{(1)}(r,\theta) + \underline{J}_{21}^{(2)}(r,\theta)\,, \tag{44}$$

- And in conductor 1:

$$\underline{J}_{12}(\rho,\varphi) = \underline{J}_{12}^{(1)}(\rho,\varphi) + \underline{J}_{12}^{(2)}(\rho,\varphi)\,. \tag{45}$$

Figures 12 and 13 show the magnitude and argument of $\underline{J}_{21}$ given by (44) on the surface of conductor 2, whereas Figures 14 and 15 show the quantities for $\underline{J}_{21}$ and $\underline{J}_{12}$ for some exemplary values of geometrical and excitation parameters.

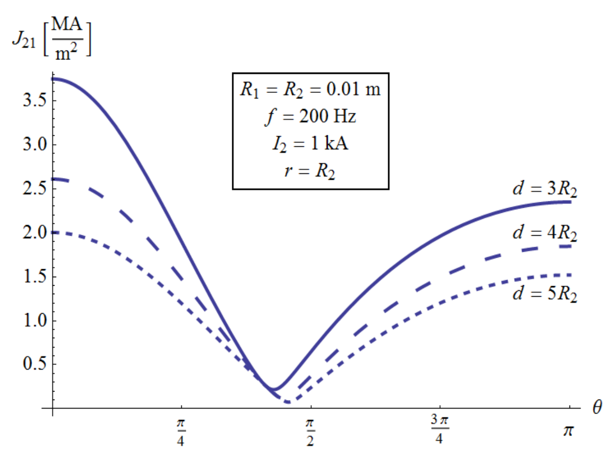

Fig. 12. Magnitude of current density given by (44) on the surface of conductor 2 for various distances d.

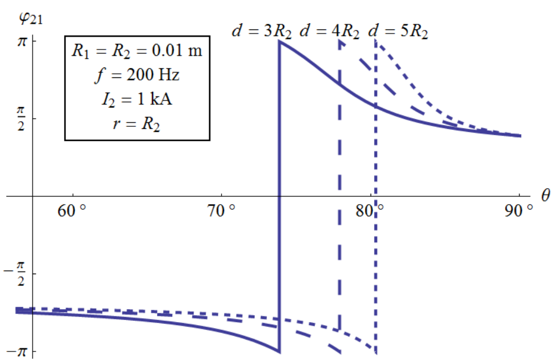

Fig. 13. Argument of current density given by (44) on the surface of conductor 2 for various distances *d*.

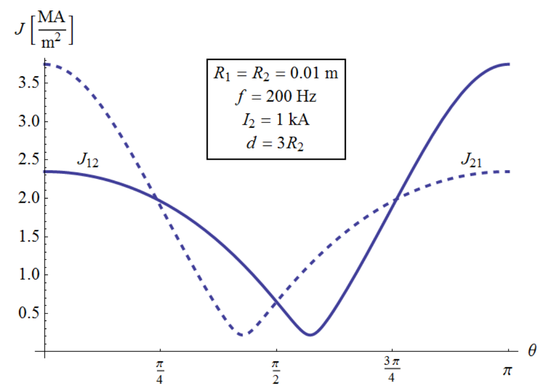

Fig. 14. Magnitude of current densities given by (44) and (45) on the surface of conductors for various distances *d*.

Table 2 presents a comparison of the results obtained via the proposed method and finite elements.

Table 2: Magnitudes of the total current densities induced at characteristic points on the surface of the conductors induced by the currents $I_1 = I_2 = 1$ kA – the first and the second approximations

$R_1 = R_2 = 0.01$ m; $d = 3R_2$; $\sigma_1 = \sigma_2 = 55 \cdot 10^6$ S/m $I = 1$ kA; $f = 200$ Hz		**Proposed Method**		**FEM**
		$J^{(1)}$ kA·m^{-2}	J kA·m^{-2}	J kA·m^{-2}
Conductor 1 $\rho = R_1$	$\varphi = 0$	2352	2354	2321
	$\varphi = \pi/2$	650	652	650
	$\varphi = \pi$	3753	3756	3714
Conductor 2 $r = R_2$	$\theta = 0$	3753	3756	3714
	$\theta = \pi/2$	650	652	650
	$\theta = \pi$	2352	2354	2321

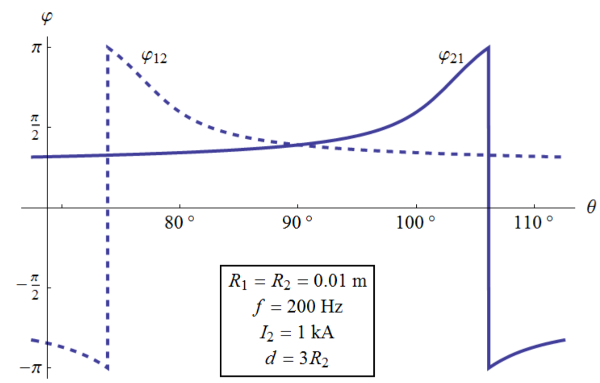

Fig. 15. Argument of current densities given by (44) and (45) on the surface of conductors for various distances *d*.

V. CONCLUSION

An analytical-numerical method for determination of the current density induced in a round conductor by magnetic field generated by a sinusoidal current in a neighboring round parallel conductor was presented in the paper. The total current density was expressed as a series of successive corrections. The solution was given in the form of infinite Fourier series.

Based on the performed calculations it can be stated the current density induced in a round conductor (without current) by current in the neighboring round conductor can be limited to the second correction. This statement seems valid even for high frequency.

Besides, the current density induced in “source” conductor by the current density previously induced in considered conductor makes an important impact on distribution of the “source” current and should not be neglected.

The proposed method can be used for any dimensions and electrical properties of the conductors and any distance between them. It is shown that the induced currents can be neglected when the distance between conductors amounts to at least four conductor diameters.

The results shown in Tables 1 and 2 confirm that the current densities calculated via the proposed method and those determined by FEMM software agree very well, indicating the correctness of the proposed approach.

The solutions for current density presented in the paper can be used to find impedances, magnetic fields, power losses and temperatures in a system of cylindrical conductors with taking into account the induced currents.

REFERENCES

[1] R. Benato and A. Paoluci, *EHV AC Undergrounding Electrical Power: Performance and Planning*, Springer-Verlag London Limited, 2010.

[2] O. Coufal, "Current density in two solid parallel conductors and their impedance," *Electrical Engineering*, vol. 96, pp. 287-297, 2014.

[3] F. Capelli and J. R. Riba, "Analysis of formulas to calculate the AC inductance of different configurations of nonmagnetic circular conductors," *Electrical Engineering*, vol. 99, pp. 827-837, 2017.

[4] A. Pagnetti, A. Xemard, F. Pladian, and C. A. Nucci, "An improved method for the calculation of the internal impedances of solid and hollow conductors with inclusion of proximity effect," *IEEE Trans. On Power Delivery*, vol. 27, pp. 2063-2072, 2012.

[5] T. Dlabać and D. Filipović, "Integral equation approach for proximity effect in a two-wire line with round conductors," *Technicki Vjesnik*, vol. 22, no. 4, pp. 1065-1068, 2015.

[6] D. Filipović and T. Dlabać, "Proximity effect in a shielded symmetrical three-phase line," *Serbian Journal of Electrical Engineering*, vol. 11, no. 4, pp. 585-59, 2014.

[7] P. Rolicz, "Eddy currents generated in a system of two cylindrical conductors by a transverse alternating magnetic field," *Electric Power Systems Research*, vol. 79, pp. 295-300, 2009.

[8] P. Jabłoński, "Cylindrical conductor in an arbitrary time-harmonic transverse magnetic field," *Przegląd Elektrotechniczny*, r. 87, no. 5, 2011.

[9] Z. Piątek, "Method of calculating eddy currents induced by the sinusoidal current of the parallel conductor in the circular conductor (in Polish)," *ZN Pol. Śl. Elektryka*, no. 75, pp. 137-150, 1981.

[10] J. R. Riba, "Analysis of formulas to calculate AC resistance of different conductors' configurations," *Electric Power Systems Research*, vol. 127, pp. 93-100, 2015.

[11] J. R. Riba, "Calculation of AC to DC resistance ratio of conductive nonmagnetic straight conductors by applying FEM simulations," *European Journal of Physics*, vol. 36, no. 5, 2015.

[12] A. Shendge, "A study on a conductor system for investigation of proximity effect," *Journal of Electromagnetic Analysis and Application*, no. 4, pp. 440-446, 2012.

[13] H. A. Aebischer and H. Friedli, "Analytical approximation for the inductance of circularly cylindrical two-wire transmission lines with proximity effect," *Advanced Electromagnetic*, vol. 7, no. 1, pp. 25-34, 2018.

[14] Z. Piątek, "Self and mutual impedances of a finite length gas-insulated transmission line (GIL)," *Electric Power Systems Research*, no. 77, pp. 191-201, 2007.

[15] Z. Piątek, *Impedances of Tubular High Current Busducts*, Polish Acad. Sci. Committee Elect. Eng. Ser. Progress in High-Voltage Technique, vol. 28, Wyd. Pol. Czest., Czestochowa, 2008.

[16] Z. Piatek, D. Kusiak, and T. Szczegielniak, "Electromagnetic field and impedances of high current busducts," in *Proceedings of the 2010 Proceedings of the International Symposium*, Wroclaw, Poland, 20-22 Sept. 2010.

[17] I. S. Gradsztejn and I. M. Ryżyk, *Tables of Integrals, Sums, Series and Products*, (in Polish), PWN, Warsaw, 1972.

Tomasz Szczegielniak was born in Konskie, Poland on Feb. 26, 1981. He received the M.S. degree from the Czestochowa University of Technology in 2006 and the Ph.D. degree from the Silesian University of Technology in 2011. Currently he is an Assistant Professor at the Institute of Optoelectronics and Measurement Systems at the Czestochowa University of Technology. His special interests are power system analysis, electromagnetic field analysis and numerical methods in engineering. He has been author or co-author of about 150 scientific papers published in Poland and abroad in conference proceedings, as monographs and in journals.

Paweł Jabłoński was born on 25 Sept. 1971 in Olesno, Poland. In 1995 he graduated from the Faculty of Electrical Engineering of Cze-stochowa University of Technology, where in 2007 he received a Doctor's degree, and in 2013 a Habilitated Doctor's degree. Currently he is an Associate Professor at the Institute of Optoelectronics and Measurement Systems. His scientific interests are electromagnetic field theory and numerical methods in solving field problems. He has written over 100 works published as books, papers in journals and conference proceedings.

Dariusz Kusiak was born on 20 Jan. 1980 in Radomsko, Poland. He graduated from the Faculty of Electrical Engineering the Czestochowa University of Technology in 2004 and received the Ph.D. degree in 2008. Currently he is an Assistant Professor at the Institute of Optoelectronics and Measurement Systems. He has written and co-written 150 works published in numerous journals and materials for both domestic as well as international scientific conferences. His scholarly interests include matters of electromagnetic fields connected with high-current lines or busducts.

Zygmunt Piatek was born in Pajeczno, Poland, on June 29, 1947. In 1972 he graduated from the Faculty of Electrical Engineering of Silesian University of Technology in Gliwice, where in 1980 he received a Doctor's degree, and in 2000 a Habilitated Doctor's degree. Since Oct. 1, 2003 he has been a Researcher and Professor at the Czestochowa University of Technology. His scientific interests include: issues referring to electromagnetic field in high current, overhead and cable low and high voltage transmission lines, earth-return circuits and impulse metal forming. He has been author or co-author of about 260 scientific papers published in Poland and abroad in conference proceedings, as monographs and in journals. He collaborates with academic and industrial centers in Poland, France, the Czech Republic and Ukraine.